2010 ASME-IMECE Conference
Vancouver, British Columbia, Canada, November 12-18, 2010

TEMPERATURE EFFECT ON DROP-WEIGHT IMPACT OF HYBRID WOVEN COMPOSITES*

Yougashwar Budhoo[a,**], Benjamin Liaw[a], Feridun Delale[a], Ramki Iyer[b], Basavaraju Raju[b]

[a] *Department of Mechanical Engineering, The City College of New York, 140th and Convent Ave., New York, NY 10031 and CUNY Graduate Center*
[b] *Tank Automotive Research, Development & Engineering Center (U.S. ARMY -TARDEC) E. 11 Mile Road, Warren, Michigan 48397-5000*

ABSTRACT

This paper investigated the effect of temperature on hybrid and non-hybrid woven composite panels (100mm×100mm×6.35mm) drop-weight impacted at five different temperatures:–60°C,–20°C, room temperature, 75°C and 125°C. The studies were conducted by combining experimental and 3-D dynamic finite element approaches. The specimens tested were made of plain-weave hybrid S2 glass-IM7graphite fibers/toughened epoxy. The composite panels were damaged using an instrumented drop-weight impact tester equipped with an environmental chamber for temperature control. The time-histories of impact-induced dynamic strains and impact forces were recorded. The damaged specimens were inspected visually and using the ultrasonic C-scan method. A 3-D dynamic finite element (FE) software package, with Chang-Chang composite damage model, was then used to simulate the experimental results of the drop-weight tests. Good agreement between experimental and FE results has been achieved. It is observed that the variation of results obtained from our experiments for the hybrid composites was very small (about 8%) when compared to those of non- hybrid composites. Also, when looking at the hybrid or non-hybrid composite, the effect of temperature at –60°C, –20°C was not significant whereas at 75°C and 125°C the results were more distinct.

INTRODUCTION

The main idea of composite material is to combine different materials to produce a new material with performance unattainable by the individual constituents. It gives flexibility to the designer to tailor the new material with properties to obtain peak performance for a particular application. The essence of the concept of composites is this: the bulk phase accepts the load over a large surface area, and transfers it to the reinforcement, which being stiffer, increases the strength of the composite. The significance here lies in the fact that there are numerous matrix materials and as many fiber types, which can be combined in countless ways to produce just the desired properties.

As the demand for materials with higher stiffness-to-weight and strength-to-weight ratios, tailoring flexibility, more resistant to harsh environment and damage tolerance arises, researchers and engineers seek to have more profound understanding of the behavior of different composites under various conditions. Investigations into woven composites have been extensive over recent years mainly because of their excellent impact resistance [1-3], dimensional stability, ease of handling etc. Some of these researches also focused on the effect of different environments, such as temperature [4-7] on the behavioral response of composite materials.

EXPERIMENTAL PROCEDURES

Materials:

The individual constituent materials combined to form the composite material studied in this research are: IM-7 graphite (IM7-GP 6000) and S2-glass (S2-4533 6000) woven fabrics in a SC-79 toughened epoxy matrix.

The IM-7 graphite woven fabric and SC-79 epoxy matrix form the non-hybrid composite called GR for short. The GR specimen contained 28 layers of graphite fabrics. For the case of the hybrid composite, it consists of a GR core, which is made up of 16 layers. This core is sandwiched between two outer laminates. Each outer laminate is made up of 9 layers of S2-glass fabrics and SC-79 epoxy. The hybrid composite is called GL/GR/GL for short.

The composite was manufactured using the vacuum assisted resin transfer molding (VARTM) technique to stack the plain woven fabrics together. The specimens were cured at

*** This work was supported by the US ARMY-TARDEC under contract # W56HZV-09-C-0569**
**** Corresponding author. Tel.: +1 646 496 6102; Fax: +1 212 650 8013.**

E-mail address: **ybudhoo00@ccny.cuny.edu** (Y. Budhoo).

Report Documentation Page

Form Approved
OMB No. 0704-0188

1. REPORT DATE	2. REPORT TYPE	3. DATES COVERED
12 NOV 2010	**N/A**	**-**

4. TITLE AND SUBTITLE
Temperature Effect on Drop-Weight Impact of Hybrid Woven Composites

5a. CONTRACT NUMBER
W56HZV-09-C0569

5b. GRANT NUMBER

5c. PROGRAM ELEMENT NUMBER

6. AUTHOR(S)
Yougashwar Budhoo; Benjamin Liaw; Feridun Delale; Ramki Iyer; Basavaraju Raju

5d. PROJECT NUMBER

5e. TASK NUMBER

5f. WORK UNIT NUMBER

7. PERFORMING ORGANIZATION NAME(S) AND ADDRESS(ES)
Department of Mechanical Engineering, The City College of New York, 140th and Convent Ave., New York, NY 10031 and CUNY Graduate Center Tank Automotive Research, Development & Engineering Center (U.S. ARMY -TARDEC) E. 11 Mile Road, Warren, Michigan 48397-5000

8. PERFORMING ORGANIZATION REPORT NUMBER

9. SPONSORING/MONITORING AGENCY NAME(S) AND ADDRESS(ES)
US Army RDECOM-TARDEC 6501 E 11 Mile Rd Warren, MI 48397-5000, USA

10. SPONSOR/MONITOR'S ACRONYM(S)
TACOM/TARDEC

11. SPONSOR/MONITOR'S REPORT NUMBER(S)
20857

12. DISTRIBUTION/AVAILABILITY STATEMENT
Approved for public release, distribution unlimited

13. SUPPLEMENTARY NOTES
Presented at the 2010 ASME-IMECE Conference Vancouver, British Columbia, Canada, November 12-18, 2010, The original document contains color images.

14. ABSTRACT

This paper investigated the effect of temperature on hybrid and non-hybrid woven composite panels (100mm¡Ñ100mm¡Ñ6.35mm) drop-weight impacted at five different temperatures:{60aC,{20aC, room temperature, 75aC and 125aC. The studies were conducted by combining experimental and 3-D dynamic finite element approaches. The specimens tested were made of plain-weave hybrid S2 glass- IM7graphite fibers/toughened epoxy. The composite panels were damaged using an instrumented drop-weight impact tester equipped with an environmental chamber for temperature control. The time-histories of impact-induced dynamic strains and impact forces were recorded. The damaged specimens were inspected visually and using the ultrasonic C-scan method. A 3-D dynamic finite element (FE) software package, with Chang-Chang composite damage model, was then used to simulate the experimental results of the drop-weight tests. Good agreement between experimental and FE results has been achieved. It is observed that the variation of results obtained from our experiments for the hybrid composites was very small (about 8%) when compared to those of non- hybrid composites. Also, when looking at the hybrid or non-hybrid composite, the effect of temperature at {60aC, {20aC was not significant whereas at 75aC and 125aC the results were more distinct.

15. SUBJECT TERMS					
16. SECURITY CLASSIFICATION OF:			17. LIMITATION OF ABSTRACT	18. NUMBER OF PAGES	19a. NAME OF RESPONSIBLE PERSON
a. REPORT **unclassified**	b. ABSTRACT **unclassified**	c. THIS PAGE **unclassified**	**SAR**	**10**	

Standard Form 298 (Rev. 8-98)
Prescribed by ANSI Std Z39-18

177^0C. Fiber volume fraction for all types was 55%. The final thickness of the specimens to be tested was 6.35mm.

Experimental setup

The low-velocity (drop-weight) impact study was conducted at five different temperatures: –60°C, –20°C, room temperature (R.T.), 75°C and 125°C. All the impact tests were performed using a drop-weight impact tester. Figure 1 shows the schematics of the experimental set-up for the low-velocity impact tests. The impact energy was fixed at 30J for all tests, which corresponds to an impact velocity of 2.9 m/s. In this study the shape of the impactor nose was hemispherical with a diameter of 16 mm. With an attached environmental chamber, an open coil heater provided the high temperatures, while the low temperatures were achieved through the use of liquid nitrogen. Specimens were clamped circumferentially with a 76 mm diameter fixture, where the clamp was considered to be a fixed-fixed support. Using a data acquisition system, the time histories of impact loads were measured and recorded using a load cell located just above the impact nose. The impact velocity was also measured by a pair of photoelectric-diodes attached to the base of the test machine. With the data acquisition system, only load (the resistive force of the specimen) vs. time and the initial impact velocity (just prior to impact) can be measured directly. Using the equations of motion, energy absorbed by the specimen, velocity of impactor and deflection at the impact center were derived and recorded.

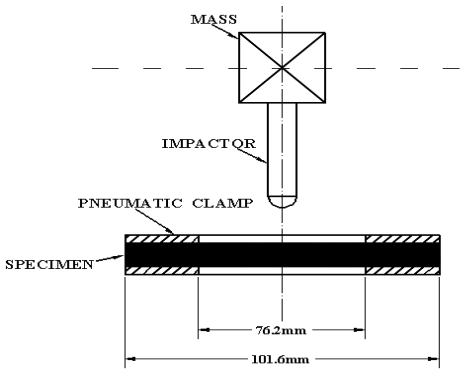

Figure 1 Schematic of the drop-weight impact test set-up

Two strain gages were mounted on the impact side (i.e., the top surface in Figure 1) of each specimen. These strain gages were mounted at a distance of 25.4 mm from the center of the composite panel, where the impactor impacted the specimens. Figure 2 shows a schematic of the strain gage orientations and locations on the specimen. SG-1 measured the radial strain while SG-2 measured the hoop strain.

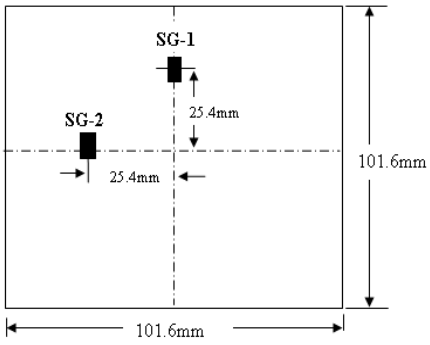

Figure 2 The locations of strain-gages on a composite specimen for drop-weight impact test

Post damage evaluation

A modular and expandable ultrasonic system was used to scan and conduct the damage evaluation for the impacted specimens. Scanning was performed using the through-transmission technique. Flat and focused 5MHz transducers (6.35mm in diameter) were used to scan these post-impacted composite specimens.

EXPERIMENTAL RESULTS

From literature review, it was found that many different factors tend to affect the damage mechanisms and damage patterns in composite materials [1-5]. Some of these factors include lay-up configuration, laminate thickness, impactor size and shape, constituent properties, temperature, impact velocity and energy, etc. To the best of authors' knowledge, no studies were done on the effect of temperature on the impact response of thick section non hybrid GR or hybrid GL/GR/GL composite material.

While there are quite a few damage mechanisms in composite materials, the most dominant form of energy dissipation is due mainly to delamination, fiber shear out and fiber breakage.

In Figures 3 and 4 the time histories of impact forces are shown. This force is the resistive force experienced by the impactor as it impacts the specimen. It can be seen that as the temperature decreases, the initial peak of the force increases. This initial peak corresponds to the initiation of damage in the composite material in the form of delamination. It can therefore be said that as temperature increases, the material becomes softer and hence the contact with impactor increases. At low temperatures, the specimen is stiffer and hence is more resistive to the advancing impactor.

Figure 3 shows the histories of impact force of the GR specimen. At –60°C,–20°C, R.T. and 75°C for GR, not only is there a drop in force after the initial peak but a few other drops along the impact force history curve later. It was realized that these specimens had back splitting after impact.

Figure 4 shows the impact force time history of the hybrid composite specimen, GL/GR/GL. It can be seen that after the initial peak force, the initial drop is less severe than that for

the GR specimen. This is due to the GL skin that is added to the GR specimen. Hybridization here tends to increase the impact performance of the GR specimen.

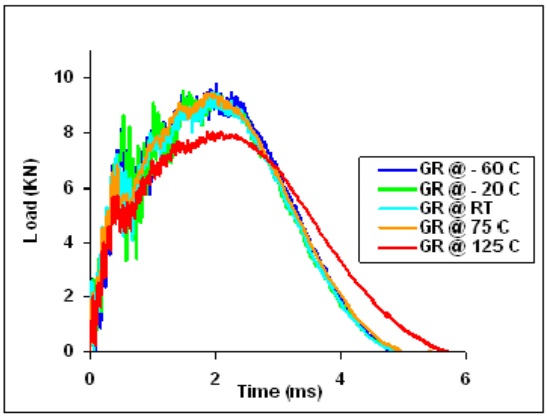

Figure 3 Time histories of the impact forces of GR composites

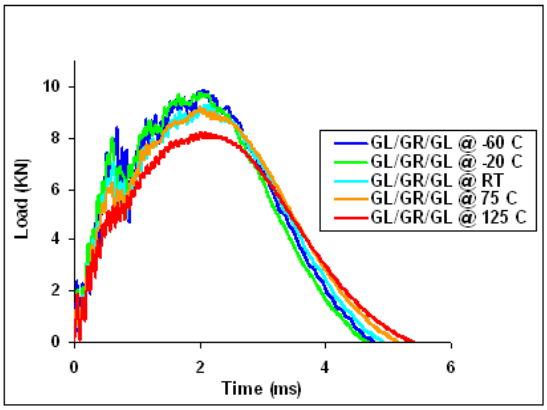

Figure 4 Time histories of the impact forces of GL/GR/GL composites

For both, the hybrid and non hybrid composites, it is seen that the total impact duration increases as the test temperature increases. This is due to the increase in ductility and deformation of the composite material. The impactor therefore spends a longer time in contact with the specimen in deforming it.

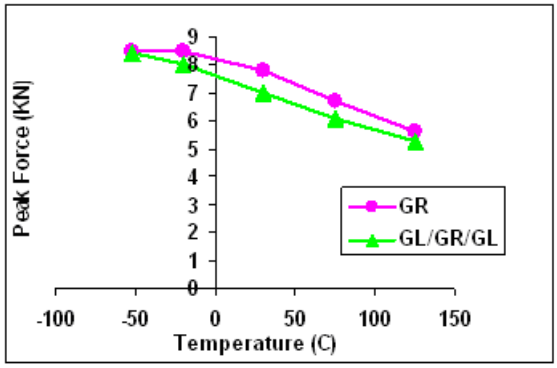

Figure 5 Initial peak force vs. temperature

In Figure 5, the initial peak force for hybrid and non hybrid composite specimens is compared. It can be seen that as the temperature increases, the initial peak force decreases. What is more interesting is the difference between the peak forces of the two composites which are responsible for damage initiation in the form of delamination. It can be seen that the hybrid composite specimen is more readily delaminated Figure 6 shows the maximum force is almost the same for both specimens.

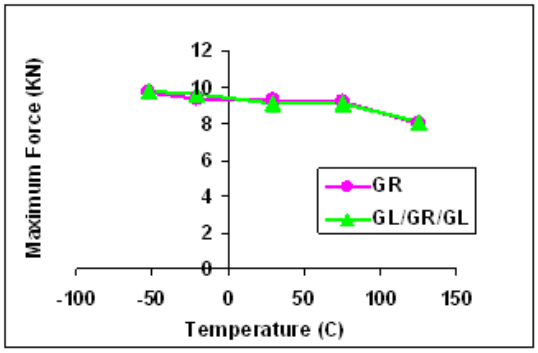

Figure 6 Maximum force vs. temperature

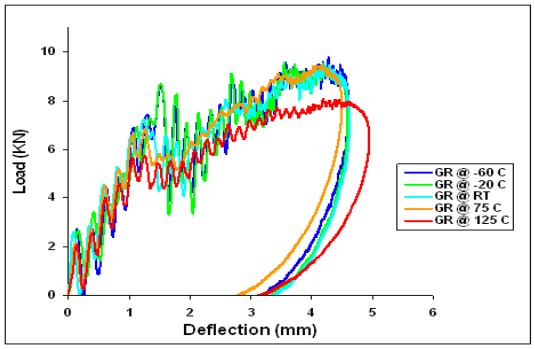

Figure 7 Contact stiffness comparison for GL/GR/GR at –60°C, –20°C, R.T., 75°C, 125°C

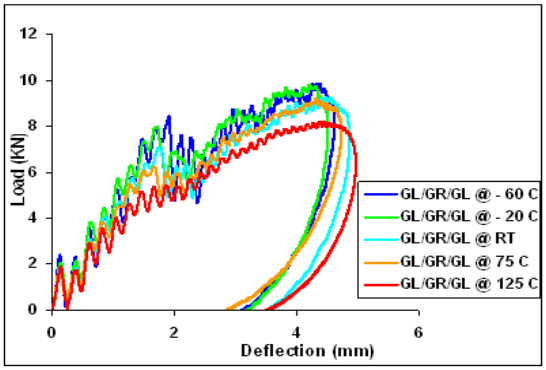

Figure 8 Contact stiffness comparison for GR at –60°C, –20°C, R.T, 75°C, 125°C

It can therefore be concluded that although the hybrid composite is more prone to delamination (this is expected because of the lower interlaminar strength between dissimilar materials), the maximum force is almost the same. At higher impact energy, it is expected that the maximum force for the

hybrid will actually become larger than that for the non hybrid composite. The GL skin therefore increases the impact resistance of GR.

Figures 7 and 8 shows the contact stiffness of the GR and the GL/GR/GL composite, respectively. It can be seen that the contact stiffness of the non hybrid is higher than that of hybrid composite. This is expected because GL has a lower stiffness and is more ductile than GR.

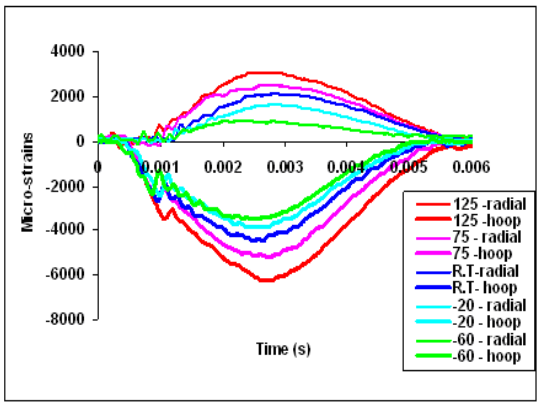

Figure 9 Dynamic strain histories for GR impacted at various temperatures

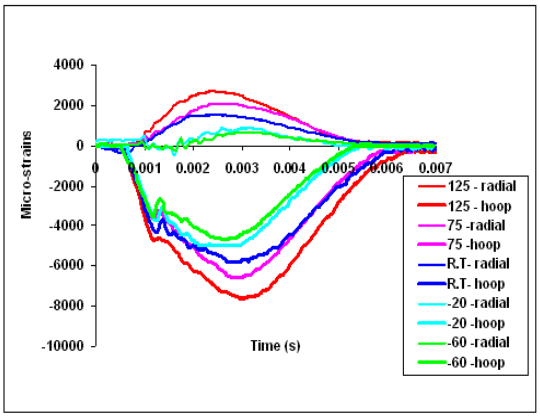

Figure 10 Dynamic strain histories for GL/GR/GL impacted at various temperatures

Figures 9 and 10 show the dynamic strain histories for the hybrid and non hybrid composites respectively. It is seen that as the temperature increases the strain rate increases. This is due to the fact that as temperature increases, the material becomes more ductile and softer hence, is more easily strained.

Figure 11 shows the images taken of the back and front of the GR specimen along with the C-scan image. It can be observed that as the temperature decreases (with the exception of 125°C) the delamination area increases.

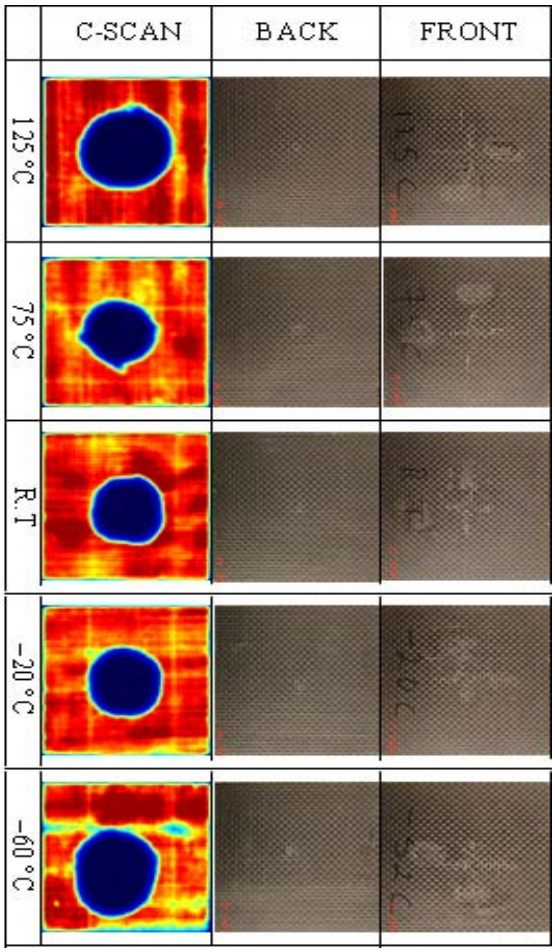

Figure 11 Optical fractographs and C-scan of non-hybrid GR composite specimens after a 30J energy level drop-weight impact at various temperatures.

At low temperatures the material is more brittle hence more of the kinetic energy of the impactor is dissipated in delaminating the specimen rather than elastically deforming the specimen. As the temperature increases, the delamination decreases because the material becomes softer and more ductile and hence has better contact with the impactor. In this case more energy of the impactor is dissipated in deforming the specimen rather than in delamination. At 125°C, the delamination area is larger than was expected and also does not follow the delamination trend. It is believed that at this temperature, the material may become unstable, since the test temperature is very close to the curing temperature (177°C) of the composite material. Images of the front of the impacted specimens show the damage pattern in the form of a cross. This is known as micro buckling of the fibers. It is considered as a secondary form of energy dissipation in the composite material. This micro buckling area increases with an increase in the test temperature due to greater deformation of the composite material, hence more buckling of the fibers.

In examining the images of the back of the GR specimen after impact, it was seen that back splitting was found on all the

specimens. It was however, less severe on the specimen where the test was conducted at 125°C as compared to the other specimens. In Figure 12, the micro buckling is clearly seen to decrease as the test temperature decreases. None of the specimen for the hybrid composite had back splitting; this is due to the fact that GL is more ductile than GR so it was able to undergo more deformation before fracture. At first glance, the C-scan image shows that the delamination area decreases with a decrease in temperature, except for –60°C. However, in examining the images more closely, it was seen that at high temperature there is compression of the material at the location of impact, and around that impact area, where the effect of the compressive stress is not

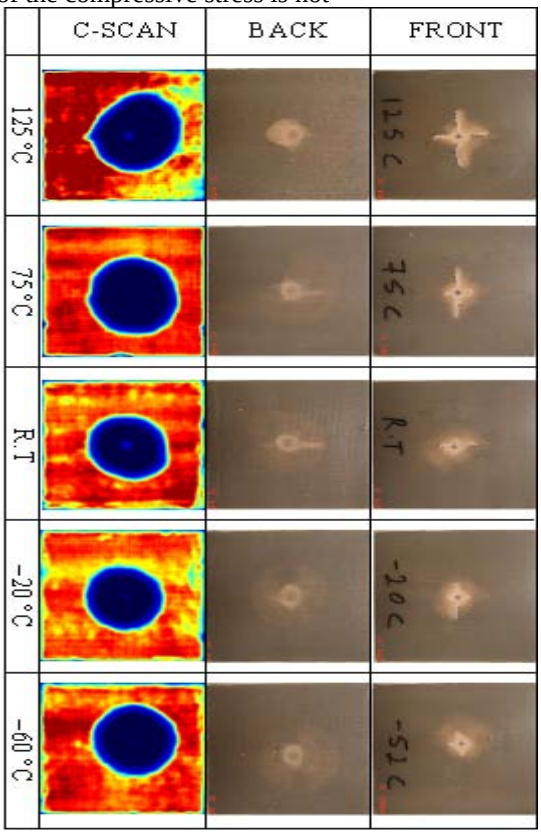

Figure 12 Optical fractographs and C-scan of non-hybrid GL/GR/GL composite specimens after a 30J energy level drop-weight impact at various temperatures

significant, there is the actual delamination area. This can be seen by the lighter shade of color at the impact location on the C-scan images. As the test temperature decreases, the compressive effect becomes smaller and hence the entire damage area revealed by the C-scan image is now the actual delamination. At high temperatures therefore, the delamination area is smaller than those for lower temperatures even though the damage area appears larger.

In Figure 13, it can be seen that the impacted surface has some fiber shear out while the back surface has splitting. The splitting is more severe at low temperatures. In Figure 14, the cross-sectional view shows no splitting on the back surface of the specimen. In the impact surface, it can also be seen that there is less damage as compared to the GR specimen. At the high temperature tests, directly below the point of impact, there is a darker core which corresponds to the compression of the specimen. At low test temperatures, it can be seen that this dark compressive core fades away.

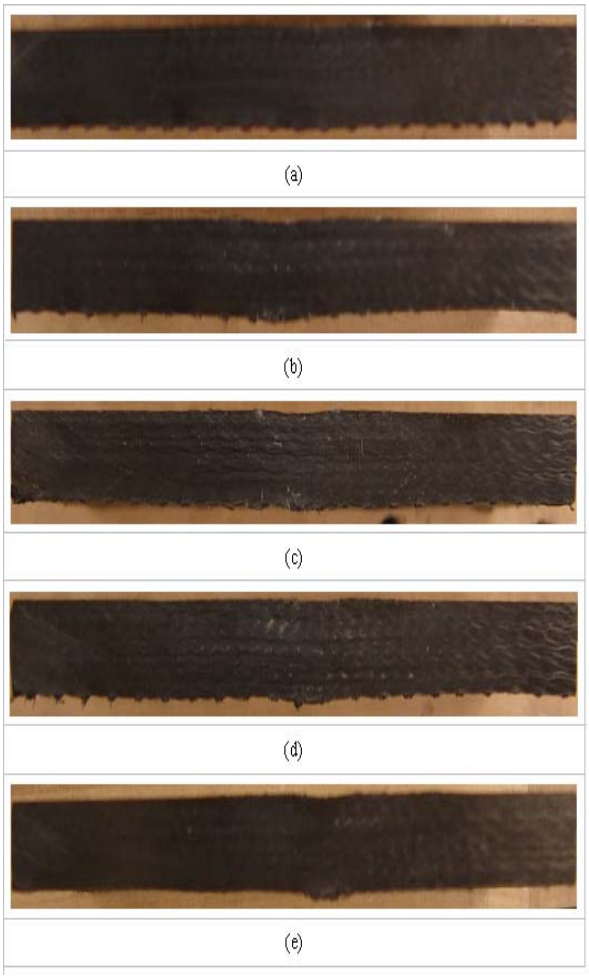

Figure 13 Optical fractographs of sectioned composites after drop impact conducted at 30 J on GR: (a) 125°C, (b) 75°C, (c) R.T. (d) –20°C, (e) –60°C

DYNAMIC FINITE ELEMENT SIMULATION

Finite element analysis (FEA) is a very useful tool in solving complex problems and also predicts the behavior of structures when actual testing may not be cost effective or practical. In this study, low velocity impact problems at various temperatures are modeled and analyzed using a 3-D nonlinear, dynamic finite element code. To validate the reliability of the model, the finite element results were compared to those obtained experimentally.

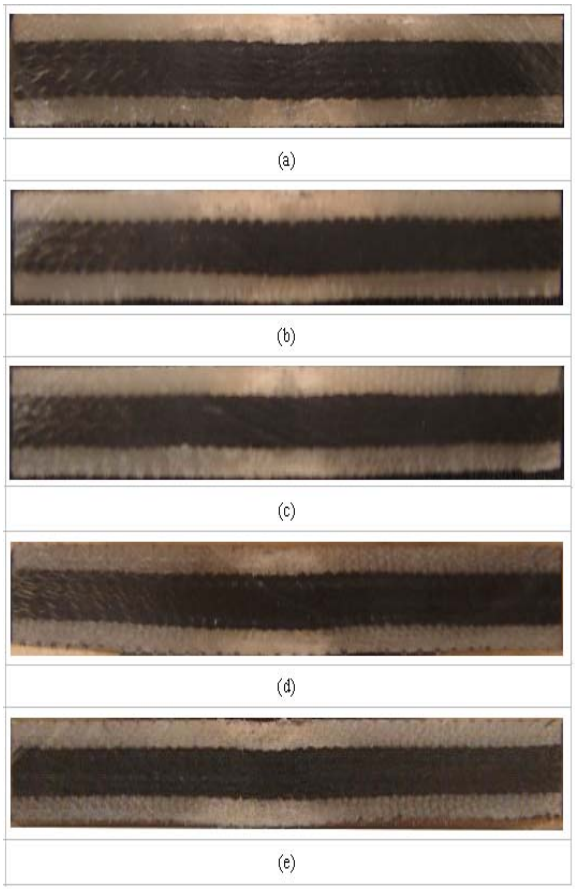

Figure 14 Optical fractographs of sectioned composites after drop impact conducted at 30 J on GL/GR/GL: (a) 125°C, (b) 75°C, (c) R.T (d) –20°C, (e) –60°C

These results include strain-time histories, contact stiffness and force. Since the geometries of the composite plate, bullet and impactor are all symmetric, it is customary that only a quarter of these parts be modeled to save computational time. All the parts were modeled using 8-node solid elements. All modeling and meshing was done using the same commercial finite element software.

Material Models

(a) MAT_ELASTIC (MAT_001): In the modeling of the impactor, the elastic material model was used. The choice of elastic model was due to the fact that the impactor stiffness is much greater than that of the specimen. In this case, no deformation is expected of the impactor but in the event of deformation, it will be elastic. So the choice of an elastic impactor seems appropriate. The choice of the more conventional rigid material model was not chosen for the impactor because in a rigid impactor, there is assumption of no deformation. This means that no energy is used up in elastically deforming the impactor and also the resulting displacement of the impactor will less accurate than that of an elastic impactor. In using MAT_ELASTIC, the required input material properties for impactor are Young's modulus, Poisson's ratio and material density.

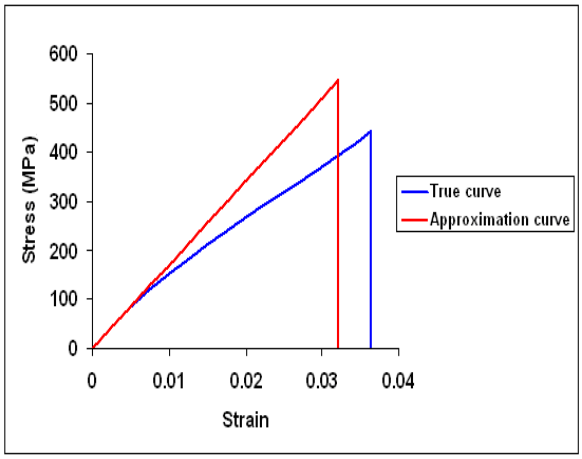

Figure 15 Linearization of non linear stress-strain curve obtained from tensile testing while maintaining strain energy

(b)MAT_COMPOSITE_DAMAGE(MAT_022):

In modeling the composite plate, MAT_022 also called the Chang-Chang composite damage model was used. This model is an orthotropic material model with optional brittle failure for composites. It requires nine material parameters to represent the composite material. From tensile testing at high temperatures, the material behavior of GR and GL/GR/GL specimens was found to be non linear. In order to use MAT_22 (best suited to describe a linear elastic behavior) to describe our materials' behavior, we consider the strain energy. Here we calculate the strain energy from the non linear stress strain behavior, and then knowing the strain energy and the initial Young's modulus, a new linear stress-strain curve is redrawn where the strain energy and Young's modulus is maintained but the failure strain and ultimate stress are changed. Figure 15 gives an example of the approximation of the true stress-strain curve for a material. The approximate curve was inputted in the finite element software instead of the true curve.

In the Chang-Chang model five material parameters are used in three possible failure criteria which are as follows:

S_1 = Longitudinal tensile strength
S_2 = Transverse tensile strength
S_{12} = Shear strength
C_2 = Transverse compressive strength
α = Non linear shear stress parameter

Here, S_1, S_2, S_{12}, and C_2 are obtained from material strength measurements and α is defined by a material shear stress-strain measurements.

The three failure critera are matrix cracking, fiber breakage and compressive failure.

(1) Matrix cracking:

$$F_{matrix} = \left(\frac{\sigma_2}{S_2}\right)^2 + \bar{\tau}$$

where $\bar{\tau} = \dfrac{\dfrac{\tau_{12}^2}{2G_{12}} + \dfrac{3}{4}\alpha\tau_{12}^4}{\dfrac{S_{12}^2}{2G_{12}} + \dfrac{3}{4}\alpha S_{12}^4}$

here σ_2 is the tensile stress in the transverse direction whereas τ_{12} is the in-plane shear stress between fibers and matrix. Failure is assumed whenever $F_{matrix} > 1$. Once this type of failure occurs, the material constants E_2 (Young's modulus in the transverse direction), G_{12} (in-plane shear modulus in the 1-2 plane), ν_{12} and ν_{21} (generalized Poisson's ratios in the 1-2 plane) are set to zero.

(2) Compressive failure:

$$F_{comp} = \left(\frac{\sigma_{12}}{2S_{12}}\right)^2 + \left[\left(\frac{C_2}{2S_{12}}\right)^2 - 1\right]\frac{\sigma_2}{S_2} + \bar{\tau}$$

Failure is assumed when F_{comp} >1. When this type of failure occurs, the material constants E_2, ν_{12} and ν_{21} are all set to zero.

(3) Fiber breakage:

$$F_{fiber} = \left(\frac{\sigma_1}{S_1}\right)^2 + \bar{\tau}$$

where σ_1 is the tensile stress in the longitudinal direction. Failure is assumed when F_{fiber} >1. After fiber breakage, E_1 (Young's modulus in the longitudinal direction), E_2, G_{12}, ν_{12} and ν_{21} are all set to zero.

MAT_ADD_EROSION (MAT_00).

This failure criterion was added to all the materials used in our modeling although it is used mostly for material models which do not have a failure or erosion criterion.
It is basically an additional criterion which when satisfied; the element is deleted from the calculation. It is a good tool to use when comparison is needed between animation and real specimen.

Contact and delamination Model

The contact between the composite layers was defined using the option,
CONTACT_AUTOMATIC_SURFACE_TO_SURFACE_TIE BREAK.
By using this contact definition, delamination between the composite layers is governed by the criterion: $\left[\dfrac{\max(0,\sigma_n)}{NFLS}\right]^2 + \left(\dfrac{\sigma_s}{SFLS}\right)^2 \geq 1$

where σ_n and σ_s are normal and shear stresses acting on the layer interface, respectively, while *NFLS* and *SFLS* are normal and shear failure strengths of the layer interface, respectively. It is assumed that delamination occurs mainly by shear failure; hence, NFLS is set to a very large number so delamination in the model is controlled by SFLS. Since SFLS is not known experimentally, it was varied in order to fit the experimental results. Additionally,
ERODING_SURFACE_TO_ SURFACE
contact model was used between the impactor and the composite. This model allows elements to be eroded when certain failure criteria are met. In this study strain-based failure criterion was used for element erosion; that is, when $\varepsilon \geq \varepsilon$erosion, the element was eroded and removed from calculation. The contact and delamination models as well as the erosion option were used for all composites.

Boundary Conditions

To model the impact event properly, the correct boundary conditions should be chosen. Preliminary simulations were carried out, and it was seen that a fixed-fixed boundary condition was the best suited to model the low velocity impact. A fixed-fixed boundary condition was therefore chosen for all the low velocity impact simulations.

Figure 16 shows the mesh of a quarter model of the plate used in simulating the drop impact test. Fine mesh around the center and course mesh away from center was used.

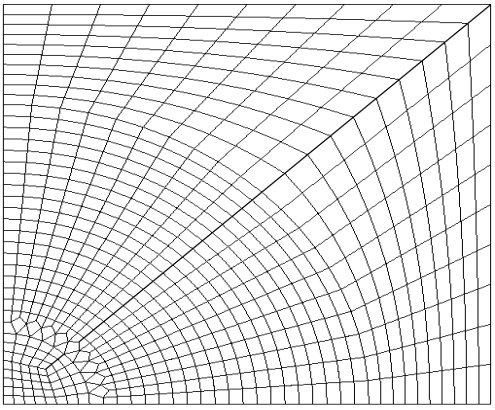

Figure 16 Quarter model of meshed plate used in drop impact simulation

Figure 17 shows the entire drop weight model of both the composite panel and the impactor for a non hybrid specimen for the low velocity impact. The material properties used to define the composite were obtained from tensile testing and are presented in Table 1.

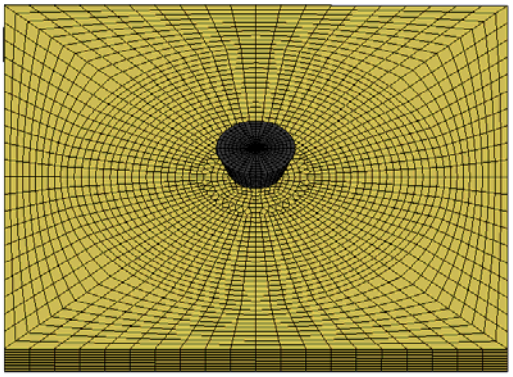

Figure 17 Mesh of entire composite plate and impactor for low velocity impact

Table 1. Key material properties used in modeling

		$E_1=E_2$ (GPa)	E_3 (GPa)	G_{12} (GPa)	$G_{13}=G_{23}$ (GPa)	ν_{12}	$\nu_{13}=\nu_{23}$	ρ (kg/m^3)
Glass	-60 °C	19.39	7.26	2.98	2.65	0.152	0.370	1766
	-20 °C	18.92	6.78	2.78	2.49	0.145	0.361	1761
	R.T	17.04	6.50	2.74	2.30	0.130	0.410	1755
	75 °C	16.13	5.85	1.89	2.03	0.128	0.436	1750
	125 °C	15.03	5.46	1.44	1.87	0.121	0.453	1744
Graphite	-60 °C	43.82	6.43	3.97	2.32	0.140	0.382	1392
	-20 °C	43.71	5.75	3.93	1.96	0.129	0.462	1387
	R.T	42.55	5.20	3.08	1.81	0.121	0.427	1381
	75 °C	41.49	3.43	1.99	1.05	0.116	0.627	1375
	125 °C	40.39	2.53	1.67	0.76	0.099	0.649	1370

Comparison of Force-Time histories

In obtaining experimental data from the data acquisition system, only the contact force i.e. resistive force of the specimen vs. time and initial impact velocity (just prior to impact) are directly measured. Therefore it can be said that the most accurate and valuable date obtained from the Dynatup 930-I data acquisition system would be the force-time histories.

Simulations were done for the hybrid and non hybrid composite at all test temperatures. But since the number of simulations turns out to be 10, and the correlation of results with experiments was good, only simulation and experimental results for highest test temperatures will be compared, i.e. for 125°C.

In Figure 18, the force-time histories were compared for the impact tests conducted on both types of composite specimen at 125°C. Comparison of FEM and experimental force-time histories shows good agreement between them. The contact duration matches quite well for the hybrid composite, however, the initiation of delamination seems to be delayed in the FEM simulation in comparison to experimental results. The FEM simulation produced a higher value for the contact force and also predicts a higher initial peak force. Predicted force-time histories of GR composites showed a contact duration that is smaller than that of the experiment. Also, the predicted maximum contact force was a little larger than that obtained from experiments. The initial peak force matches quite well with experimental results.

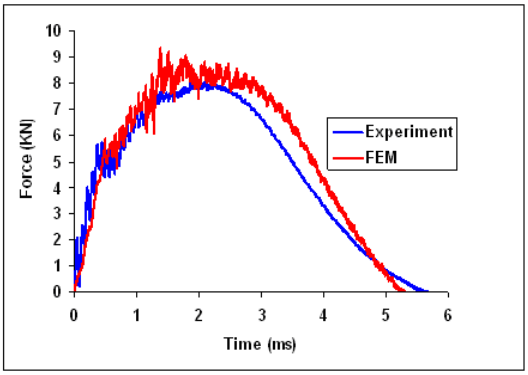

(a)

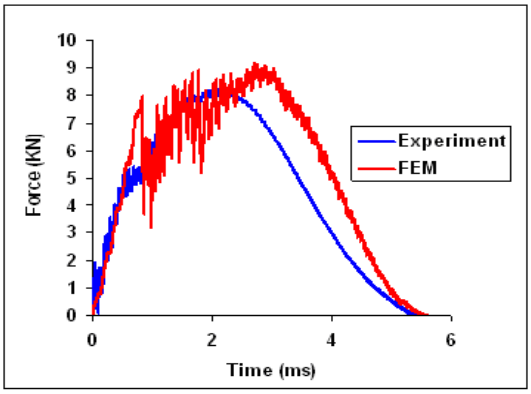

(b)

Figure 18 Comparison of FEM and experimental force-time histories for (a) GR, (b) GL/GR/GL, composite plates impacted at 125°C

Comparison of contact stiffness

Figure 19 shows the comparison of the contact stiffness between experiment and FEM. The predicted curve matches quite well with the experimental curve especially in the initial portion. After damage initiates, there is a little variation in the results between the two curves, especially in the unloading portion. Again this can be explained by the approximation of the material stiffness in material modeling and also the idealization of the boundary conditions.

Comparison of Strain-Time histories

In Figure 20 the experimental and FEM dynamic surface strain histories are shown. The experimental curves are a lot smoother than those generated by FEM. This can be explained by the fact that experimental strain measurements were obtained through a strain gage amplifiers, where actual readings might have been filtered. One reason why the FEM results were not very smooth is due to the fact that the contact between layers was held by the nodes of the contacting layers. As the material was being stressed, stress build up continues at the contacting nodes until the failure criterion for delamination is reached. When delamination occurs, the stress at the nodes suddenly drops and the crack progresses further to near-by

nodes in contact where the stress builds up again until delamination occurs. Then the process gets repeated again.

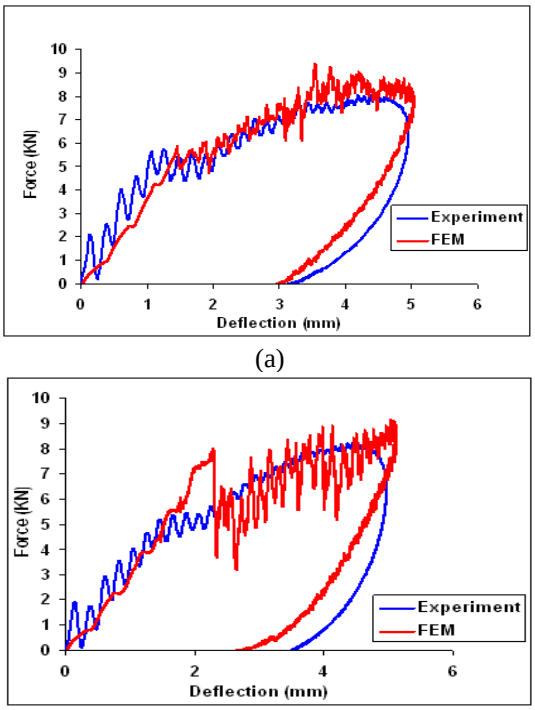

(a)

(b)

Figure 19 Comparison of FEM and experimental contact stiffness for (a) GR, (b) GL/GR/GL composites impacted at 125°C

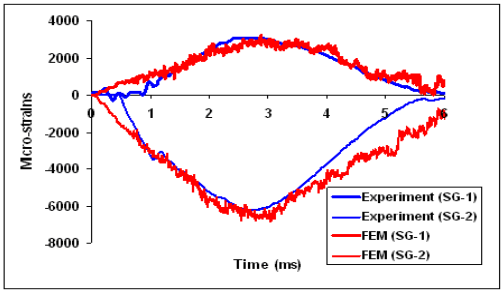

(a)

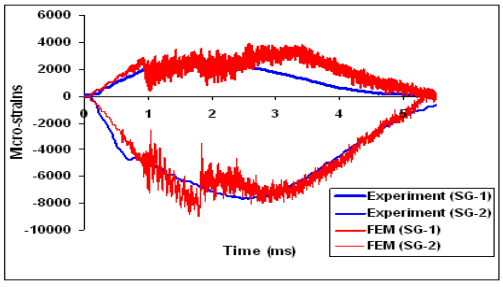

(b)

Figure 20 Comparison of dynamic strain histories of (a) GR (b) GL/GR/GR/GL composite plates impacted at 125°C

This rise and fall in stress cause the strain output to have a lot of oscillations. In order to increase the smoothness of the strain curve, the specimen should be modeled with finer meshes where the nodes will be closer to each other and delamination will have a smoother transition. The comparison in strain outputs in Figure 20 above are in good agreement with each other, but the model couldn't predict the initial portion of the strain curve quite well for the non hybrid specimen.

Comparison of post-impact damage patterns

In Figure 21 the post impact damage of the cross section between the test specimen and FEM model shows good agreement in respect to the deformation and damage patterns. In Figure 22, the FEM model agrees well with the actual specimen, however the model predicts a slightly higher permanent deformation than that of the actual specimen.

Figure 21 (a) Comparison of post impact damage patterns of (a) experimental and (b) FEM results for drop-weight tests at 125 °C for GR using 16mm hemispherical impactor

Figure 22 (a) Comparison of post impact damage patterns of (a) experimental and (b) FEM results for drop-weight tests at 125 °C for GL/GR/GL

CONCLUSIONS

From the results discussed above, the following conclusions can be drawn:

(1) As the test temperature decreases, the delamination area increases.

(2) After the initial peak of the force-time curves, if there is large oscillation in the curve, then there is back splitting of the specimen.

(3) Hybridization tends to improve the impact resistance of GR.

(4) The FE model incorporated with MAT_22 (Chang-Chang material model) can successfully simulate the low velocity impact tests.

(5) The validity of the FE model was confirmed with the use of experimental results such as; force, energy, strain histories and post-impact damage patterns. The experimental and FE predicted results agreed sufficiently for low-velocity impact tests. The model however, could be improved by introducing a material model that accurately captures the actual material behavior.

REFERENCES

[1] Sevkat E., Liaw B., Delale F., Raju B.B., Drop-weight impact of plain-woven hybrid glass–graphite/toughened epoxy composites. Composites Part A: Applied Science and Manufacturing, Vol. 40, Issue 8, August 2009, pp. 1090-1110

[2] Sevkat E., Liaw B., Delale F., Raju B.B., Effect of repeated impacts on the response of plain-woven hybrid composites. Composites Part B: Engineering, 2010. DOI:10.1016/j.compositesb.2010.01.001

[3] Wu E. and Chang L.C., Woven glass/epoxy laminates subject to projectile impact, International Journal of Impact Engineering, Vol. 16, 1995, No. 4, Pages 607-619.

[4] Hirai Y., Hamada H. and Kim J.K., Impact response of woven glass-fabric composites- II. Effect of temperature., Composites Science and Technology, Vol. 58, Issue 1, January 1998, pp. 119-128

[5] Im K.H, Cha C.S, Kim K.S, Yang I.Y., Effects of temperature on impacts damages in CFRP composite laminates. Composites Part B, Vol. 32, 2001, pp. 669–82.

[6] Parlevliet P.P, Bersee H.E.N, and Beukers A, Residual stresses in thermoplastic composites- A study of the literature- Part 1: Formation of residual stresses. Applied Science and Manufacturing, Vol. 37, Issue 11, November 2006, pp. 1847-1857

[7] Dlouhy I., Chlup Z., Boccaccini D. N., Atiq S. and Boccaccini A. R., Fracture behaviour of hybrid glass matrix composites: thermal ageing effects, Composites Part A: Applied Science and Manufacturing, Vol 34, Issue 12, December 2003, pp 1177-1185.

[8] Jones M. R., Mechanics of Composite Materials, Sec. 4.5, Thermal and Mechanical Stress Analysis, Edwards Brothers, Ann Arbor, MI, 1998.

[9] Naik N. K., Sekher C.Y. and Meduri S., Damage in woven-fabric composites subjected to low-velocity impact, Composites Science and Technology, Vol 60, Issue 5, April 2000, pp 731-744